WCTE 2020
WORLD CONFERENCE ON TIMBER ENGINEERING
SANTIAGO, CHILE | 24 - 27 AUGUST

MACRO MODELING TECHNIQUE FOR INTEGRALLY-ATTACHED TIMBER PLATES: SENSITIVITY ANALYSIS

Aryan Rezaei Rad[1,*], Henry Burton[2], Yves Weinand[1]

ABSTRACT: Using the Integral Mechanical Attachment (IMA) technique, a new macroscopic model has recently been introduced to simulate the structural behavior of segmented timber plates. The macro model is based on employing only beam and spring elements, which aims to reduce the computational time associated with the database generation and analysis runtime. Despite its simplicity, the model provides a reliable modeling approach. In the current paper, the sensitivity of the behavior of the macro model to variations in the geometry of timber plates is investigated. Three types of timber plates with rectangular, parallelogram and irregular geometries are designed and subjected to the sensitivity analysis. The corresponding macro models are subjected to out-of-plane loads. Constructing the corresponding continuum Finite Element (FE) models, the deformation of the macro models is compared to that the FE models. The deformed shape obtained from the macro model was similar to that of the FE model with an approximately 5% error.

KEYWORDS: Timber Plates, Macro model, Finite Element model, Wood-Wood Connections, Sensitivity analysis.

1 INTRODUCTION

The proliferation of interactive modeling tools and visual programming languages have given rise to the Computer-Aided Design (CAD) in digital architecture. Accordingly, algorithmic programming and parametric geometric processing have overcome the limitations of traditional CAD. This, in particular, has enabled the generation of custom-defined geometries, which is beyond the human manual ability. Furthermore, numerical models that include the geometrical and mechanical properties of the system under consideration are often used in structural analysis and design. Spurred by recent advancements in open-source computational platforms, numerical simulation techniques have been widely embedded in the Computer-Aided Engineering (CAE). Moreover, developments in the production of engineered timber products such as Laminated Veneer Lumber (LVL) panels, the use of Computer Numerical Control (CNC) machines for digital fabrication, and the application of robotic arms for assembly of building components have resurrected the Integral Mechanical Attachment (IMA) technique in timber plates. The framework leads to the design of Integrally-Attached Timber Plate (IATP) structures with custom-defined forms, ranging from standard shapes [1][2] to spatial free-form geometries [3].

IATP structures have been widely researched over the last decade. The primary areas of focus were on geometry generation, architectural design, and digital fabrication [4]. Furthermore, the mechanical characterization of IATPs at the connection scale has been widely studied [5–7]. Moreover, physical experiments and numerical solutions using the conventional approaches (i.e. employing continuum Finite Element (FE) models) have been conducted [8–10]. Despite the potential of such detailed models in providing enhanced simulation capabilities and capturing the stress-strain response and local failure modes, it is required to develop modeling strategies that can be used by practitioners. This is mainly due to the fact that refined FE models are detailed, complex, require a high level of sophistication, and typically computationally expensive. Accordingly, a macroscopic model for IATPs has recently been introduced by Rezaei Rad et al. [11]. The macro model employs only beam and spring elements to simulate the global behavior of IATPs. Accordingly, the level of details associated with the modeling process of IATP

[1] **Aryan Rezaei Rad**, École Polytechnique Fédérale de Lausanne (EPFL), School of architecture, civil and environmental engineering, Laboratory for timber construction (IBOIS), GC H2 711, Station 18, 1015-Lausanne, Switzerland, aryan.rezaeirad@epfl.ch

[2] **Henry Burton**, University of California Los Angeles (UCLA), Department of civil and environmental engineering, United States, hvburton@ucla.edu

[3] **Yves Weinand**, École Polytechnique Fédérale de Lausanne (EPFL), School of architecture, civil and environmental engineering, Laboratory for timber construction (IBOIS), Switzerland, Yves.Weinand@epfl.ch

components is adapted to simplify the analysis and design. Consequently, the macro model proposes an efficient model that can be used in structural engineering practice. In the current paper, the sensitivity of the macro model to variations in the geometry of timber plates is evaluated. The macro models and the corresponding FE models using shell elements are constructed and subjected to out-of-plane loads.

2 INTEGRAL MECHANICAL ATTACHMENT (IMA) TECHNIQUE

Using timber as a material with high machinability, together with the CNC machinery technique to mill different joint geometries and computer-aided design, digital fabrication has re-defined a new construction framework in timber plate structures. In light of this, Robeller [12] introduced an efficient automatic production of wood-wood connections in thin timber plate structures. The wood-wood connections, which are also referred to as Integral Mechanical Attachment (IMA) or carpentry joints, rely on direct force-transfer between timber components. Therefore, IMAs establish connections between timber elements through their form, instead of using additional connectors such as adhesives, screws, nails, drift pins, bolts, and welding. Dovetail-shaped (Fig. 1a) and Through-Tenon (TT) joints (Fig.1b) are mostly used to construct timber plate structures. In these connections, there is only one translation vector in a 3D space to (dis)assemble adjacent elements. Given this consideration, the term "1DOF assembly technique" is used to describe the joinery process. In fact, the term "1DOF" refers to the relative deformation between the inter-connected timber components, which is restricted to a single direction.

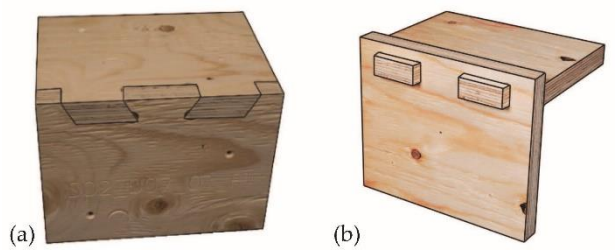

Figure 1: *Integral Mechanical Attachments (IMAs)*

The six kinematics degrees of freedom (DOFs) associated with the 3D continuum geometry of the joint region are identified. These DOFs are shown in Fig. 2. According to the identified kinematics, the mechanical performance assessment of the IMAs has been the subject of research investigations in recent years. Rezaei Rad et al. [13] experimentally investigated the performance of IMAs under tensile loads (Fig. 3a). Furthermore, the edgewise (in-plane) behavior of IMAs was researched by Rezaei Rad et al. [14] (Fig. 3b). Recently, the flatwise behavior of IMAs, which corresponds to the out-of-plane response of the IATP element in their joint region, has been studied in Rezaei Rad et al. [15] (Fig. 3c). Moreover, a basis for characterizing the moment-rotation behavior of the joints under flexural moments have been widely investigated by Roche [16], Nguyen et al. [10], and Rezaei Rad et al. [1] (Fig. 3d).

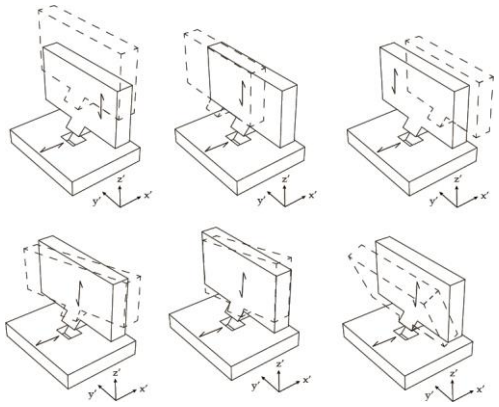

Figure 2: *six kinematics degrees of freedom (DOFs) associated with the 3D continuum geometry of IMAs*

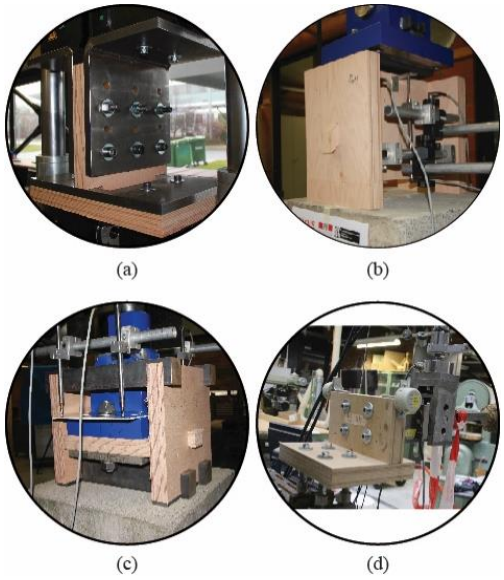

Figure 3: *Experimental tests used to study the (a) tensile, (b) edgewise, (c) flatwise, and (d) flexural behavior of IMAs*

Quantitative evaluations of the observed load-deformation behavior of the TT joints are provided in Table 1. Using the European standards EN 26891 [17] and EN 12512 [18], the quantitative performance evaluation is described in terms of key design parameters such as strength, design stiffness (slip modulus), and ductility capacity.

Table 1: *Mechanical behavior of IMAs [1][13][14][15]*

DOF	Description	K_{slip}	Max. Strength	Ductility
1	Tensile behavior	0.66 N/mm	14.65 E3 N	1.07
2	Edgewise behavior	8.6 N/mm	33.3 E3 N	3.7
3	Flatwise behavior	7.17 N/mm	27.5E3 N	2.94
4	Flexural behavior	4.5E5 N.mm/°	3.2E6 N.mm	2.07

The kinematic DOFs associated with the 3D continuum geometry of the joint region is idealized using a link element. The element consists of six different springs, which capture the tensile, edgewise (in-plane) and flatwise (out-of-plane) force deformation and flexural, and torsional moment-rotation behavior of the joint. The joint region and the equivalent spring elements used in the two-node link element is shown in Fig. 4.

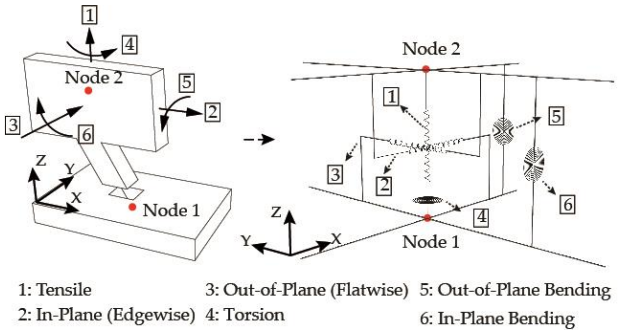

Figure 4: *Two-node link element with six springs used to simulate IMAs*

3 INTEGRALLY-ATTACHED TIMBER PLATE (IATP) STRUCTURES

By providing multiple tabs along the edge of a plate and multiple slots along with its mate, a so-called "edgewise" connection between two adjacent timber plates is achieved [12]. The term "interlocked" is used because the assembly sequence of multiple timber plates prevents separation of the structure. Accordingly, a new design framework has recently been proposed by Robeller and Weinand [19] and Robeller et al. [4] which implements the 1DOF IMA technique in the design of non-standard free-from timber plate structures. The design framework aims to include the geometry generation, the definition of the assembly sequence, construction plan, and fabrication process within the design workflow of Integrally-Attached Timber Plate (IATP) structures. A doubly-curved arch including two layers of interconnected timber shells has been designed as a case study by the Laboratory for Timber Construction (IBOIS)[4]. Having a Miura-Ori pattern [20], the arches serve as spatial roofs for an industrial building similar to Eladio Dieste [21]. Fig. 5 shows an IATP structure constructed by ANNEN SA[5] in Manternach, Luxembourg.

The target surface of a free-form structure is transformed into a target geometry. Accordingly, the configuration of the timber plates is determined. The system includes the assembly of multiple 4-sided boxes. Each box consists of top and bottom plates (denoted as T_i and B_i in Fig. 5) and two cross plates (denoted as CL_i and, CT_i in Fig. 5). Within each box, the tenons are located along the edges of the T_i and B_i plates and their mates are located in the CL_i and CT_i plates. Each box is then connected to its neighbor with only the TT joints. Each timber box is labeled with a normal vector. The collective set of normal vectors within a structure can be algorithmically determined so that they comply with the target surface to achieve the desired geometry.

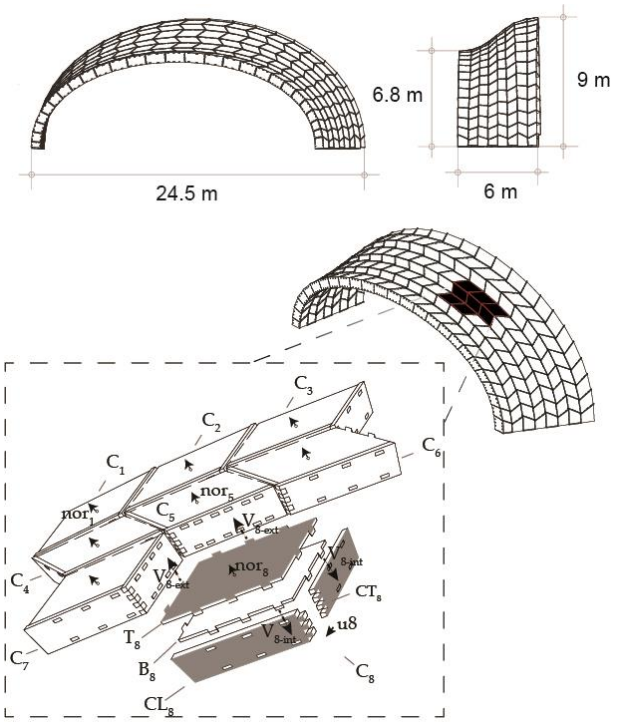

Figure 5: *Integrally-Attached Timber Plate (IATP) Structures*

4 MACROSCOPIC MODEL FOR TIMBER PLATE STRUCTURES

In general, the structural analysis of complex systems requires model simplifications. Macroscopic models are accordingly used in numerical simulations. These models adopt a series of one-dimensional elements such as springs or beam elements to simulate the behavior of shells or plates. The technique is used as an alternative to the refined continuum-based FE method. The macro modeling technique primarily aims to reduce the computational expense while maintaining the accuracy of the response simulation. Furthermore, macro models can reduce the overall complexity and enhance the interpretability of numerical analyses. Fig. 6 schematically shows the difference between the number of elements used in a typical continuum FE and macro model of an IATP structure with 5X3 boxes.

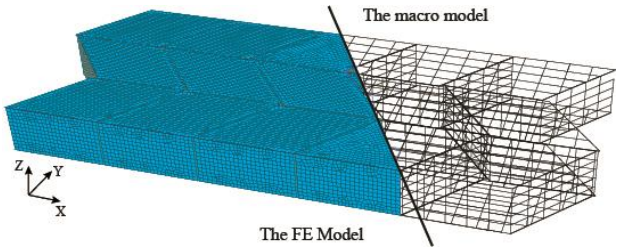

Figure 6: *FE vs. macro model in IATP structures*

[4] https://www.epfl.ch/labs/ibois/

[5] http://www.annen.eu/

The introduction and formulation of a macroscopic model for a specific structural system depend on multiple parameters related to the construction material (e.g. timber, concrete, masonry, steel), geometric properties (i.e. the form of the structure), structural features (e.g. rigidity of connections, boundary conditions, etc.), kinematic assumptions (in-plane behavior, out-of-plane behavior of components), and fabrication and construction limitations (i.e. CNC routers, robotic assembly vs. manual assembly, on-site casting vs. bespoke prefabrication, etc.). Taking all of these factors into account, only those degrees of freedom (DOFs) that contribute significantly to component and system deformations are included in the macro model formulation.

Macro models have been developed for different types of structural systems including masonry vaults [22], infilled frame structures [23], frame structures with steel plates [24], reinforced concrete (RC) shear wall structures [25], timber frames with wood sheathings and metal fasteners [26], timber folded plate surfaces [8], and recently, free-form IATP structures [11].

The macro model associated with an IATP element (Fig. 7a) is shown in Fig. 7b. It consists of inner beams along the fiber parallel (Fig. 7c) and fiber-perpendicular directions (Fig. 7d), shear springs along the fiber parallel (Fig. 7e) and fiber-perpendicular directions (Fig. 7f), uniaxial tension-compression springs distributed along with the boundary elements (Fig. 7g-h), multiple two-node link elements representing the semi-rigidity of the joints (Fig. 7j), and boundary elements (Fig. 7j) [11]. The boundary and inner beam elements are pin-ended. The former is articulated and free to rotate about its local y' and z' axes, and the latter is only free to rotate about the local z' axis.

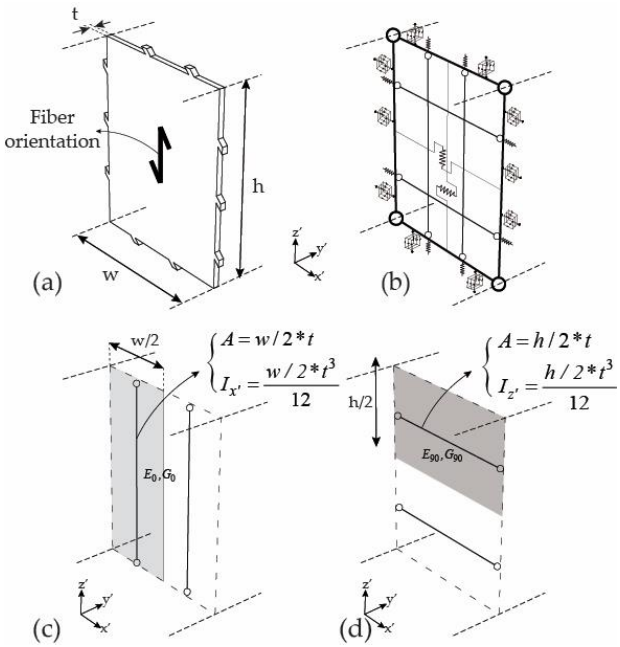

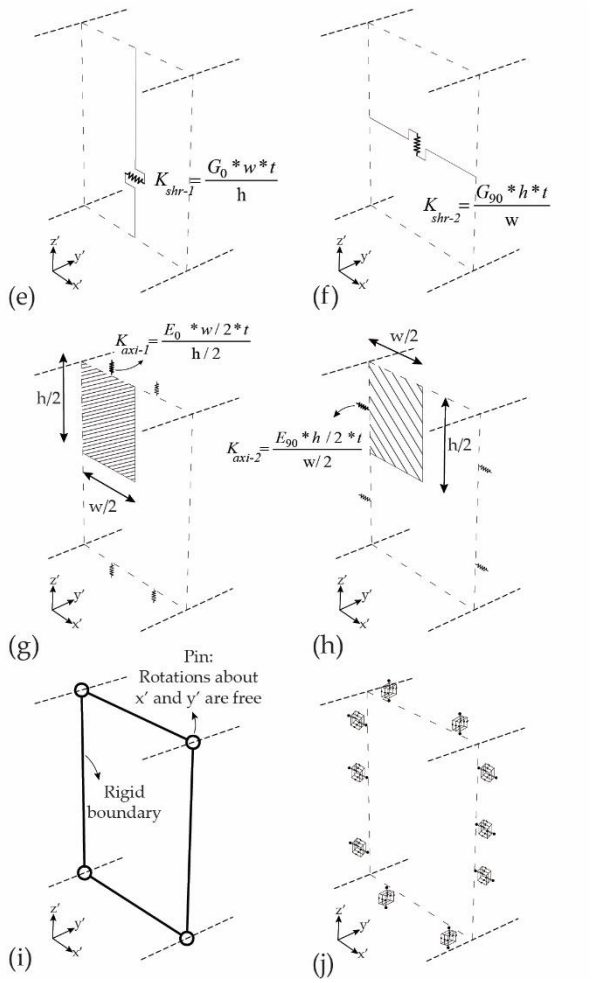

Figure 7: *The macro model in IATP structures*

The inner beam elements provide the out-of-plane flexural stiffness while the shear springs and the uniaxial tension-compression springs provide the in-plane stiffness. Since the interaction between the IMA-boundary elements is included in the edgewise spring elements, the boundary elements are modeled as rigid. This makes the macro model independent of the geometry of the plate.

To develop the geometry of the macro model, the fabrication contours of a custom-defined quadrilateral 3D IATP element and the associated mid-surface are identified. The macro model is then generated from the mid surface (Fig. 8a) in accordance with the following steps: (1) The four corner nodes (Fig. 8b) are used to construct a planar polygon, which serves as the boundary element of the macro model, (2) the location of the IMAs in the boundary elements are identified (Fig. 8c), (3) the polygon is divided into equal segments along the fiber-parallel (Fig. 8d) and fiber-perpendicular directions (Fig. 8e) and inner lines are added at the segment interfaces. These lines serve as the inner beams for the macro model, and (4) the boundary elements are divided at the intersections and the end nodes of the inner beams, joints, and the corner nodes are connected (Fig. 8f).

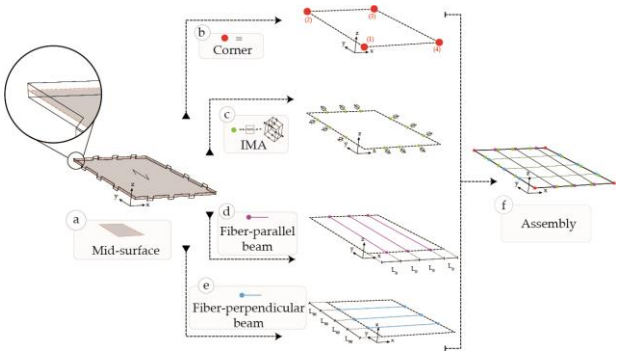

Figure 8: *(a) Isometric view of timber plate represented with fabrication contours and the associated mid-surface, (b) polygon created with the mid-surface corner nodes, (c) identifying and locating the TT joints in the boundary element, (d-e) dividing the polygon along the fiber-parallel and fiber-perpendicular directions and inserting the inner beams, (f) establishing boundary elements using the nodes associated with steps (b) to (e).*

5 SENSITIVITY ANALYSIS

The sensitivity of the behavior to variations in the geometry of the macro models under out-of-plane loads is investigated in this study. Given that the macro model is valid for 4-sided planes [11], three main geometries are considered for the timber plates. In particular, a rectangular plate, a parallelogram plate, and an irregular quadrilateral with non-parallel edges are designed, where the associated dimensions are shown in Fig. 9a to Fig. 9c, respectively. The geometric configuration of these plates is based on the average dimensions of the elements in the full-scale prototypes reported in [4,10,11] and designed according to Eurocode 5.

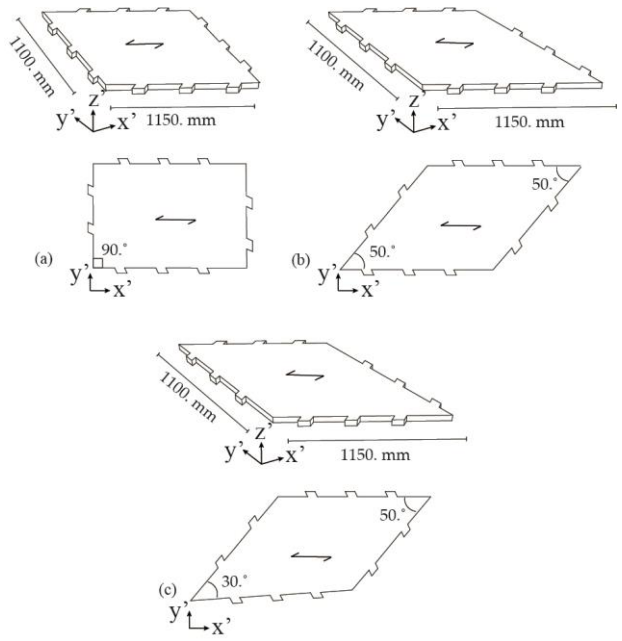

Figure 9: *The macro model in IATP structures*

The macro models associated with the defined geometries are constructed. The inner beams are constructed by dividing the timber plates into four equal segments along the fiber-parallel and fiber-perpendicular directions. The tributary area associated with each beam element is accordingly computed and assigned. Beech BauBuche Laminated Veneer Lumber (LVL) [27] is employed as the construction material, and consequently, the orthotropic material properties (Table 2) are assigned to the inner beams. For the sake of simplification, the same division used to build the inner beams is employed to allocate the uniaxial tension-compression springs. The properties of the shear springs are also computed according to the net cross-section per each fiber orientation and the shear properties of the Beech LVL panels (Table 2). The mechanical properties of the components of the macro model for the three pre-defined geometries are shown in Fig. 10.

The macro models are subjected to 9.0 kN load which is along the out-of-plane direction (local z'). This load corresponds to the Ultimate Limit State (ULS) of the IMAs in the IATP element according to Rezaei Rad et al. [15]. The out-of-plane load is applied to the timber plates at the location of the five IMAs identified as Z1 to Z5 in Fig. 11. Furthermore, each timber plate is constrained at the rest of the IMAs within the IATP element which are shown in Fig. 11.

Table 2: *Material Properties of beech BauBuche* [27]

Symbol	Description	Value (N/mm²)
E_0	Modulus of elasticity, fiber-parallel	13200.
E_{90}	Modulus of elasticity, fiber-perpendicular	2200.
G_0	Shear modulus, fiber-parallel	820.
G_{90}	Shear modulus, fiber-perpendicular	430.

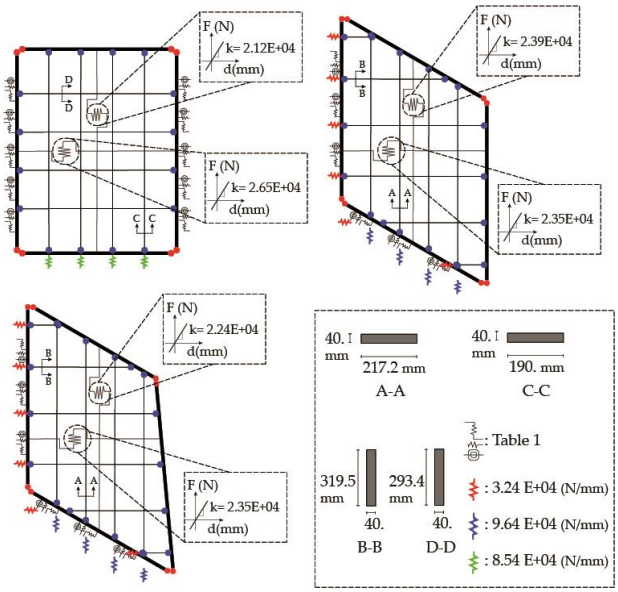

Figure 10: *The macro model in IATP structures*

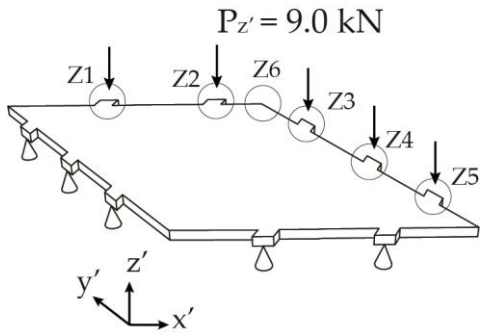

Figure 11: *The macro model in IATP structures*

The continuum FE models are built in ABAQUS/CAE [28]. The mid surface of the timber plate is used to represent the panel, which is then simulated by a shell element sub-divided into meshes under a linear elastic response. The quad type using finite strain S4R with a seed size of 20 mm is used for the meshes. Employing Beech BauBuche LVL, orthotropic material properties (Table 2) are assigned to the poly-surface shell elements. The IMAs are simulated using the Bushing element. The continuum FE model is schematically shown in Fig. 12.

The macro models are built in OpenSees version 2.5.0 [29]. For the inner beams and boundary elements, the elastic beam-column element is employed from the OpenSees library. Furthermore, a uniaxial material with elastic properties with infinite stiffness is assigned to the boundary elements. Moreover, the IMAs are modeled using the two-node link element from the OpenSees library. The macro model is schematically shown in Fig. 12.

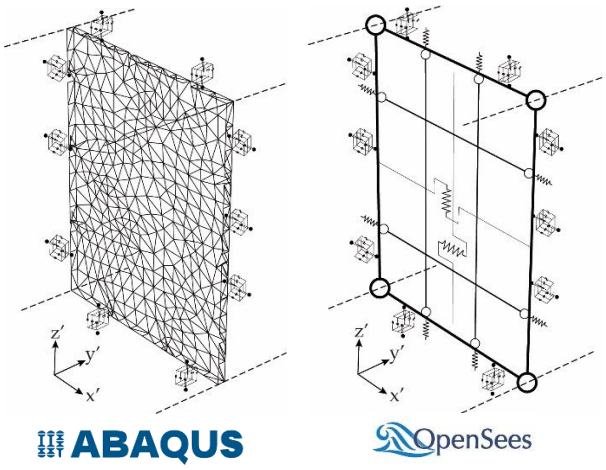

Figure 12: *The macro model in IATP structures*

The performance of the FE and macro models, in terms of the displacement values, are assessed in the six pre-defined locations (Z1 to Z6 in Fig. 11) for the three types of the timber plates. Accordingly, for the rectangular, parallelogram, and irregular timber plates, the performance of the macro models in the stations Z1 to Z6 are given in Table 3 to Table 5, respectively.

Table 3: *Vertical displacement at joints under out-of-plane load for the rectangular timber plate*

Zones	Displacement (mm)		Error (%)
	FE	Macro	
1	65.3	62.3	4.6
2	95.0	93.1	2.0
3	83.2	77.7	6.6
4	49.8	46.8	6.0
5	15.9	16.1	1.6
6	124.2	123.8	0.3

Table 4: *Vertical displacement at joints under out-of-plane load for the timber plate with parallelogram geometry*

Zones	Displacement (mm)		Error (%)
	FE	Macro	
1	78.5	68.7	12.5
2	101.1	97.7	3.4
3	82.3	84.9	3.2
4	54.2	55.1	1.7
5	25.1	25.2	0.4
6	115.1	122.8	6.7

Table 5: *Vertical displacement at joints under out-of-plane load for the irregular timber plate with non-parallel edges*

Zones	Displacement (mm)		Error (%)
	FE	Macro	
1	47.5	39.6	16.6
2	78.5	69.9	11.0
3	68.2	68.6	0.6
4	47.3	47.8	1.1
5	25.9	26.2	1.2
6	94.2	85.15	9.6

The results show that the deformed shape obtained from the macro model is in good agreement with the one obtained from the FE model with an average difference of 3.5%, 4.6%, and 6.7% for the rectangular, parallelogram, and irregular timber plates, respectively. These differences are attributed to the different element formulations in the macro and FE models. In fact, in the FE formulation, the nodal degrees of freedom for each finite element is coupled. However, in the macro model, separate (uncoupled) springs are used to model the shear, flexural, and axial behavior of the plate. In other words, in the FE model, the rigidity of the element is distributed over the plate, while in the macro model, the rigidity is concentrated in a specific number of discrete elements. This leads to differences in the curvature along the element for the FE and macro models. Nevertheless, simulating the out-of-plane kinematics with multiple beam elements can distribute the out-of-plane stiffness over the plate surface with an acceptable degree of accuracy. This has been shown in Fig. 12, where the deformation of the macro model for the irregular timber plate is compared to the corresponding Finite Element (FE) model.

The results indicate that the difference between the behavior of the macro and FE models increases when the geometry changes from the rectangular plate to the irregular plate. In fact, changing the geometry from the

rectangular plate to the irregular quadrilateral, the flexural stiffness of the local axes x' and y' affects each other. While this interaction can be captured quite well by the FE continuum model, the macro model faces challenges in capturing this kinematic mainly because of the discrete modeling approach. This, in particular, make the macro model sensitive to the resolution of the inner beams.

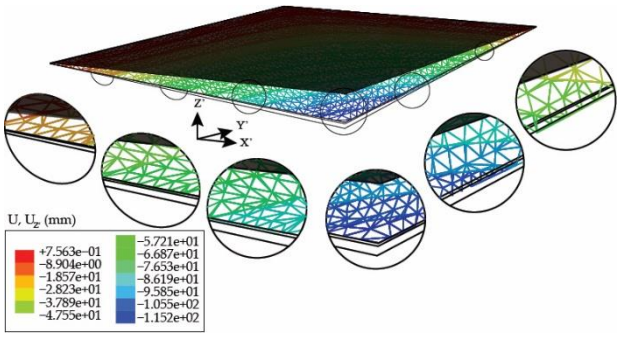

Figure 13: *The macro model in IATP structures*

6 CONCLUSIONS

Using the recently-developed macroscopic model for Integrally-Attached Timber Plate (IATP) elements, the performance of timber plates with different geometries is studied in this paper. It is concluded that the out-of-plane stiffness of the component can be simulated using multiple beam elements parallel and perpendicular to the fiber orientation. Furthermore, to have a better understanding of the local behavior of IATPs when the macro model is used, it is recommended to increase the number of the inner beams. Despite its simplicity, the macro model is robust and can simulate the behavior of IATPs. Using only beams and spring elements, the macro model analysis converged with no numerical instabilities. The creation of the model database, as well as the computational time required for analysis, was significantly less than the time required in the continuum FE models. It is also concluded that the macro model can simulate timber plates with symmetric geometries with a minimum amount of error. Nevertheless, the irregular timber plates with asymmetric geometries can be simulated with an acceptable degree of accuracy.

7 ACKNOWLEDGEMENT

The supports of the National Centre of Competence in Research (NCCR) Digital Fabrication (https://dfab.ch/) (agreement ID #51NF40141853) and the Laboratory for Timber Construction (IBOIS) at École Polytechnique Fédérale de Lausanne (EPFL) are acknowledged (https://www.epfl.ch/labs/ibois/).

8 REFERENCES

[1] A. Rezaei Rad: "Mechanical Characterization of Integrally-Attached Timber Plate Structures: Experimental studies and macro modeling technique", Doctoral thesis, École Polytechnique Fédérale de Lausanne (EPFL), 2020. https://doi.org/10.5075/EPFL-THESIS-8111

[2] A.C. Nguyen, Y. Weinand: "Development of a spring model for the structural analysis of a double-layered timber plate structure with through-tenon joints", *in: 2018 World Conf. Timber Eng. WCTE 2018, Seoul*, 2018. https://doi.org/https://doi.org/20.500.11850/314629

[3] C. Robeller, M. Konaković, M. Dedijer, M. Pauly, Y. Weinand: "Double-layered timber plate shell", Int. J. Sp. Struct. 32, 160–175, 2017. https://doi.org/10.1177/0266351117742853.

[4] C. Robeller, M. Konakovic, M. Dedijer, M. Pauly, Y. Weinand: "A Double-layered Timber Plate Shell - Computational Methods for Assembly, Prefabrication and Structural Design", *in: Adv. Archit. Geom. 2016, vdf Hochschulverlag AG, Zürich, Switzerland*, pp. 104–122. 2016 https://doi.org/10.3218/3778-4.

[5] M. Dedijer, S. Roche, Y. Weinand: "Shear resistance and failure modes of edgewise Multiple Tab-and-Slot Joint (MTSJ) connection with dovetail design for thin LVL spruce plywood Kerto-Q panels", *in: WCTE 2016 - World Conf. Timber Eng., Vienna University of Technology, Vienna, Austria*, pp. 1516–1523, 2016

[6] S. Roche, G. Mattoni, Y. Weinand: "Rotational Stiffness at Ridges of Timber Folded-plate Structures", Int. J. Sp. Struct. 30, 153–167, 2015. https://doi.org/10.1260/0266-3511.30.2.153.

[7] S. Roche, C. Robeller, L. Humbert, Y. Weinand: "On the semi-rigidity of dovetail joint for the joinery of LVL panels", Eur. J. Wood Prod. 73, 667–675, 2015. https://doi.org/10.1007/s00107-015-0932-y.

[8] A. Stitic, A. Nguyen, A. Rezaei Rad, Y. Weinand: "Numerical Simulation of the Semi-Rigid Behaviour of Integrally Attached Timber Folded Surface Structures", Buildings. 9, 55, 2019. https://doi.org/10.3390/buildings9020055.

[9] A. Stitic, C. Robeller, Y. Weinand: "Experimental investigation of the influence of integral mechanical attachments on structural behaviour of timber folded surface structures", Thin-Walled Struct. 122, 314–328, 2018. https://doi.org/10.1016/j.tws.2017.10.001.

[10] A.C. Nguyen, P. Vestartas, Y. Weinand: "Design framework for the structural analysis of free-form timber plate structures using wood-wood connections", Autom. Constr. 107, 102948, 2019. https://doi.org/10.1016/J.AUTCON.2019.102948.

[11] A. Rezaei Rad, H. V. Burton, Y. Weinand: "Macroscopic Model for Spatial Timber Plate

Structures with Integral Mechanical Attachments", J. Struct. Eng. (United States). 146, 2020. https://doi.org/10.1061/(ASCE)ST.1943-541X.0002726.

[12] C. Robeller: "Integral Mechanical Attachment for Timber Folded Plate Structures", Doctoral thesis, École Polytechnique Fédérale de Lausanne (EPFL), 2015. https://doi.org/10.5075/epfl-thesis-6564.

[13] A. Rezaei Rad, H. Burton, Y. Weinand: "Performance assessment of through-tenon timber joints under tension loads", Constr. Build. Mater. 207, 706–721, 2019. https://doi.org/10.1016/J.CONBUILDMAT.2019.02.112.

[14] A. Rezaei Rad, Y. Weinand, H. Burton: "Experimental push-out investigation on the in-plane force-deformation behavior of integrally-attached timber Through-Tenon joints", Constr. Build. Mater. 215, 925–940, 2019. https://doi.org/10.1016/J.CONBUILDMAT.2019.04.156.

[15] A. Rezaei Rad, H. Burton, Y. Weinand: "Out-of-plane (flatwise) behavior of through-tenon connections using the integral mechanical attachment technique", Constr. Build. Mater. 262, 2020. https://doi.org/10.1016/j.conbuildmat.2020.120001.

[16] S. Roche: "Semi-Rigid Moment-Resisting Behavior of Multiple Tab-and-Slot Joint for Freeform Timber Plate Structures", Doctoral thesis, École Polytechnique Fédérale de Lausanne (EPFL), 2017. https://doi.org/doi:10.5075/epfl-thesis-8236.

[17] CEN (European Committee for Standardization): "EN 26891: Timber structures - Joints made with mechanical fasteners - General principles for the determination of strength and deformation characteristics", Brussels, Belgium, 1991.

[18] CEN (European Committee for Standardization): "EN 12512: Timber structures – test methods – cyclic testing of joints made with mechanical fasteners", Brussels, Belgium, 2001.

[19] C. Robeller, Y. Weinand: "Fabrication-aware Design of Timber Folded Plate Shells with Double Through Tenon Joints", *in: D. Reinhardt, R. Saunders, J. Burry (Eds.), Robot. Fabr. Archit. Art Des., Springer International Publishing*, pp. 166–177, 2016. https://doi.org/10.1007/978-3-319-26378-6_12.

[20] T. Tachi: "Geometric Considerations for the Design of Rigid Origami Structures", *in: Int. Assoc. Shell Spat. Struct. Symp.*, International Association for Shell and Spatial Structures, Shanghai, 2010.

[21] R. Pedreschi, D. Theodossopoulos: "Eladio Dieste: resistance through form" *in: 1st Int. Conf. Struct. Archit. ICSA 2010, University of Edinburgh, Edinburgh, United Kingdom*, pp. 797–805, 2010.

[22] B. Pantò, F. Cannizzaro, S. Caddemi, I. Caliò: "3D macro-element modelling approach for seismic assessment of *historical* masonry churches", Adv. Eng. Softw. 97, 40–59, 2016. https://doi.org/10.1016/j.advengsoft.2016.02.009.

[23] I. Caliò, B. Pantò: "A macro-element modelling approach of Infilled Frame Structures", Comput. Struct. 143, 91–107, 2014. https://doi.org/10.1016/j.compstruc.2014.07.008.

[24] I.-R. Choi, H.-G. Park: "Hysteresis Model of Thin Infill Plate for Cyclic Nonlinear Analysis of Steel Plate Shear Walls", J. Struct. Eng. 136, 1423–1434, 2010. https://doi.org/10.1061/(ASCE)ST.1943-541X.0000244.

[25] Y. Bao, S.K. Kunnath: "Simplified progressive collapse simulation of RC frame-wall structures", Eng. Struct. 32, 3153–3162, 2010. https://doi.org/10.1016/j.engstruct.2010.06.003.

[26] H. Burton, A. Rezaei Rad, Z. Yi, D. Gutierrez, K. Ojuri: "Seismic collapse performance of Los Angeles soft, weak, and open-front wall line woodframe structures retrofitted using different procedures", Bull. Earthq. Eng. 17, 2059–2091, 2019. https://doi.org/10.1007/s10518-018-00524-w.

[27] H.J. Blaß, J. Streib: "Ingenious hardwood: BauBuche Beech laminated veneer lumber Design assistance for drafting and calculation in accordance with Eurocode 5", Pollmeier Massivholz GmbH & Co.KG, Creuzburg, Germany, 2017. https://www.pollmeier.com/en/downloads/design-manual.html#gref.

[28] Dassault Systemes, SIMULIA Abaqus/CAE, 2012.

[29] S. Mazzoni, F. McKenna, M. Scott, G. Fenves: "OpenSees [Computer Software]: The open system for earthquake engineering simulation", 2013. http://opensees.berkeley.edu/.